

1 Convective heat and mass transfer modelling at air-porous material interfaces: 2 overview of existing methods and relevance

3
4 Thijs Defraeye ^{a*}, Bert Blocken ^b, Dominique Derome ^c, Bart Nicolai ^a, Jan Carmeliet ^{d,e}

5
6 ^a VCBT / MeBioS, Department of Biosystems, Katholieke Universiteit Leuven, Willem de Croylaan 42, 3001 Heverlee,
7 Belgium

8 ^b Building Physics and Services, Eindhoven University of Technology, P.O. Box 513, 5600 Eindhoven, The Netherlands

9 ^c Department of Civil and Mechanical Engineering, Swiss Federal Laboratories for Materials Testing and Research
10 (Empa), Überlandstrasse 129, 8600 Dübendorf, Switzerland

11 ^d Chair of Building Physics, Swiss Federal Institute of Technology Zurich (ETHZ), Wolfgang-Pauli-Strasse 15, 8093
12 Zürich, Switzerland

13 ^e Laboratory for Building Science and Technology, Swiss Federal Laboratories for Materials Testing and Research
14 (Empa), Überlandstrasse 129, 8600 Dübendorf, Switzerland

15

16 **Keywords**

17 convective transfer coefficient; conjugate modelling; porous material; computational fluid dynamics; drying; air flow

18

19 **Abstract**

20 Accurate predictions of convective heat and mass transfer at air-porous material interfaces are essential in many
21 engineering applications, one example being optimisation of industrial drying processes with respect to energy
22 consumption and product quality. For porous-material modelling purposes, simplified convective transfer coefficients
23 (CTCs) are often used to avoid explicit air-flow modelling. Alternatively, conjugate models have been introduced
24 recently and are being more widely used. Conjugate modelling has the advantage that it does not require the use of
25 CTCs or of the heat and mass transfer analogy. Instead, these CTCs can be identified a-posteriori. In this study, an
26 overview of the existing methods to predict convective heat and mass transfer at air-porous material interfaces is given,
27 with a specific focus on conjugate modelling. The improved accuracy of this approach is indicated based on two case
28 studies, namely hygroscopic loading and convective drying. A large spatial and temporal variability of the CTCs is
29 found by means of conjugate modelling. This approach provides increased accuracy, which is especially relevant for
30 complex flow problems, such as in industrial drier systems. However, the sensitivity to the convective boundary
31 conditions can be limited in some cases, e.g. for hygroscopic loading. Instead of improving accuracy significantly here,
32 conjugate modelling will rather impose an additional modelling effort, which often requires conjugate model code
33 development as these models are not readily available. Before embarking on a conjugate modelling study, it is advised
34 to perform a sensitivity analysis with respect to the convective boundary conditions: in some cases, sufficient accuracy
35 can be obtained using empirical CTCs from literature.

36

37

* Corresponding author. Tel.: +32 (0)16321618; fax: +32 (0)16322966.
E-mail address: thijs.defraeye@biw.kuleuven.be

Defraeye T., Blocken B., Derome D., Nicolai B., Carmeliet J., (2012), Convective heat and mass transfer modelling at air-porous material interfaces: overview of existing methods and relevance, *Chemical Engineering Science* 74, 49-58. <http://dx.doi.org/10.1016/j.ces.2012.02.032>

39 **Nomenclature**

40

41	D_{PM}	thickness of porous material (m)
42	D_{GB}	thickness of gypsum board (m)
43	$g_{v,w}$	convective water vapour flux at the air-porous material interface/wall (kg/m ² s)
44	H	channel height (m)
45	L_{PM}	length of porous material (m)
46	$p_{v,ref}$	reference vapour pressure (Pa)
47	$p_{v,w}$	vapour pressure at the air-porous material interface/wall (Pa)
48	$q_{c,w}$	convective heat flux at the air-porous material interface/wall (W/m ²)
49	Re	Reynolds number
50	R_{BL}	vapour diffusion resistance of boundary layer (m/s)
51	R_{GB}	vapour diffusion resistance of gypsum board (m/s)
52	t	time (s)
53	t_{tot}	total time (s)
54	T	temperature (K or °C)
55	T_{ref}	reference temperature (K or °C)
56	T_w	temperature at the air-porous material interface/wall (K or °C)
57	T_{wb}	wet bulb temperature (K or °C)
58	U_b	bulk air speed (m/s)
59	x	coordinate (m)
60	y	coordinate (m)

61

62 *Abbreviations*

63	avg	surface-averaged
64	CDRP	constant drying rate period
65	CFD	computational fluid dynamics
66	CHTC	convective heat transfer coefficient
67	CMTC	convective mass transfer coefficient
68	CTC	convective transfer coefficient
69	DDRP	decreasing drying rate period
70	EPDM	effective penetration depth model
71	HAM	heat-air-moisture
72	RH	relative humidity
73	TP	transition period

74

75 *Greek symbols*

76	$\delta_{v,GB}$	water vapour diffusion coefficient of gypsum board (s)
----	-----------------	--

77

78 *Subscripts*

79	BL	boundary layer
----	----	----------------

80	CDRP	constant drying rate period
81	GB	gypsum board
82	PM	porous material
83	ref	reference condition
84	v	water vapour
85	w	wall/air-porous material interface
86		
87		

88 **1. Introduction**

89 Convective heat and mass transfer from porous materials is of interest for many engineering applications, such as: (1) a
90 wide range of industrial drying applications (Mujumdar, 2006; Putranto et al., 2011), e.g. the production of building
91 materials (concrete, brick, gypsum board, etc.; e.g. Suresh et al., 2001; Murugesan et al., 2001), food processing
92 (Scheerlinck et al., 2000, 2001; Hoang et al., 2000, 2003; Kaya et al., 2006; De Bonis and Ruocco, 2008; Lamnatou et
93 al., 2009; Lamnatou et al., 2010) or wood and paper production (Erriguible et al., 2006; Younsi et al., 2008; Kowalski,
94 2010; Kowalski and PawLowski, 2011). The vast majority of these drying processes still occur convectively and are
95 very energy consuming operations. Optimisation of the drying process is particularly required to enhance processing
96 efficiency, in terms of energy usage and production time, without compromising the product quality, for example by
97 excessive shrinkage or warping; (2) outdoor hygrothermal analysis of building envelopes and components from the
98 perspective of design of durable building envelope systems and preservation of cultural heritage. Here knowledge on
99 the convective exchange is required, for example to analyse thermal performance (e.g. Palyvos, 2008; Blocken et al.,
100 2009; Defraeye et al., 2010, 2011a, 2011b), to determine the drying of facades wetted by wind-driven rain (e.g. Blocken
101 and Carmeliet, 2004; Blocken et al., 2007), or to analyse several physical, chemical and biological weathering processes
102 (e.g. Poupeleer et al., 2006a, 2006b); (3) indoor hygrothermal analysis related to indoor climate and comfort, mould
103 growth risk, moisture buffering (Steehan et al., 2009a; Carmeliet et al., 2011), preservation of valuable historical
104 objects such as paintings (Steehan et al., 2009b), energy consumption related to (de)humidification of the air, etc.; (4)
105 analysis of volatile organic compound (VOC) emissions to indoor air (Yang et al., 2001). Since the majority of the
106 aforementioned applications involve moisture transport (i.e. liquid and vapour), this paper will focus on water (H₂O) as
107 the mass transfer component. A generalisation to other substances is straightforward.

108
109 In addition to experimental research on these convective transfer mechanisms (e.g. Belhamri and Fohr, 1996; Iskra et
110 al., 2009), several numerical modelling approaches have been developed to model the coupled heat and moisture
111 transport in porous materials, such as pore network models (e.g. Prat, 1993; Carmeliet et al., 1999; Yiotis et al., 2001)
112 or macroscopic models (e.g. Ben Nasrallah and Perre, 1988; Cloutier et al., 1992; Janssen et al., 2007; Moonen et al.,
113 2010). In these models, the convective heat and mass exchange with the environment is usually modelled by means of
114 convective heat and mass transfer coefficients, i.e. CHTCs and CMTCs, respectively. These convective transfer
115 coefficients (CTCs) relate the convective heat and moisture flux normal to the wall ($q_{c,w}$ and $g_{v,w}$), i.e. the air-porous
116 material interface, to the difference between the wall temperature (T_w) or vapour pressure at the wall ($p_{v,w}$) and a
117 reference temperature (T_{ref}) or vapour pressure ($p_{v,ref}$), for example the approach flow conditions:

118
$$CHTC = \frac{q_{c,w}}{T_w - T_{ref}} \quad (1)$$

119
$$CMTC = \frac{g_{c,w}}{p_{v,w} - p_{v,ref}} \quad (2)$$

120 The fluxes are assumed positive away from the porous material. CTCs however account for the convective exchange in
121 a quite simplified way (Defraeye et al., 2012): (1) CTCs are often estimated by means of empirical correlations with the
122 air speed, where these correlations were mostly derived for simplified configurations, such as flat plates; (2) The spatial
123 variation of CTCs along the surface and especially their temporal variation are often not accounted for; (3) CMTCs are
124 often estimated from CHTCs by using the heat and mass transfer analogy (Chilton and Colburn, 1934), which only
125 applies under strict conditions (no radiation, no coupling between heat and mass transfer, analogous boundary

126 conditions, etc.); (4) CTCs are strongly dependent on the reference conditions (T_{ref} and $p_{v,ref}$), but the location where
127 these are evaluated is generally chosen rather arbitrary for complex flow problems. Due to these simplifications, the use
128 of such CTCs can seriously compromise the accuracy of the air-side convective heat and mass transfer predictions for
129 certain applications, one of them being convective drying of porous materials (Defraeye et al., 2012).

130
131 Since convective heat and mass transfer from porous materials involves transport both in the air and in the porous
132 material, it is actually a conjugate transport problem and should be considered likewise in numerical modelling, thus by
133 accounting for two domains: the air and the porous material. Thus, instead of using the well-established CTCs,
134 explicitly resolving heat and mass transport in the air, in addition to resolving heat and mass transport in the porous
135 material, is advised since it is inherently more accurate. Several approaches towards such conjugate modelling of
136 convective exchange processes have been proposed in the past two decades and will be discussed in this paper. Note
137 however that a reduced accuracy of the imposed convective boundary conditions (e.g. by using CTCs) in porous-
138 material modelling does not necessarily disturb a reliable simulation (Belhamri and Fohr, 1996), for example when heat
139 and mass transport at the porous material-side governs the transport kinetics. The level of complexity with which the
140 air-side convective exchange processes have to be accounted for in numerical models and the impact on the accuracy of
141 the simulation results are thus important questions to be answered when dealing with convective transfer problems.

142
143 This study aims to clarify some of the aforementioned issues regarding convective transfer predictions, and their impact
144 on numerical modelling. First, an overview of different modelling approaches and previous studies for convective heat
145 and mass transfer for porous materials is given, with a specific focus on conjugate modelling, and their advantages and
146 limitations are discussed. Second, the relevance of accurate numerical modelling of convective exchange processes is
147 indicated by means of two (conjugate) case studies, namely hygroscopic loading and convective drying of porous
148 materials. Third, a discussion on convective heat and mass transfer predictions and the need for conjugate modelling is
149 presented.

150

151 **2. Overview of numerical modelling approaches**

152 Numerically solving convective heat and mass transfer problems implies that both the transport in the air and in the
153 porous material are modelled (and solved), which can be done at several levels of complexity in both media. For
154 porous-material modelling, the following approaches are commonly used:

- 155 • Effective penetration depth model (EPDM, Cunningham, 1992).
- 156 • Shrinking core models, also called receding front models (e.g. Luikov, 1975; Hashimoto et al., 2003).
- 157 • Macroscopic continuum models for coupled multiphase heat and mass transport in porous materials. Three
158 approaches exist: (1) the phenomenological approach (Philip and De Vries, 1957; Luikov, 1966); (2) the
159 approach relying on mixture theory (e.g. Bowen, 1980); (3) the volume-averaging approach at the microscopic
160 scale (see Whitaker, 1977, 1998).
- 161 • Pore-network models (e.g. Prat, 1993; Carmeliet et al., 1999; Yiotis et al., 2001), of which an overview can be
162 found in Blunt (2001) and Prat (2002).

163

164 From the perspective of porous-material models, the degree of conjugate modelling is determined by the way in which
165 the heat and mass transport in the air is accounted for. The most commonly used approaches are:

- 166
- 167
- 168
- 169
- 170
- 171
- 172
- 173
- 174
- 175
- 176
- 177
- 178
- 179
- 180
- 181
- 182
- 183
- 184
- 185
- 186
- 187
- 188
- 189
- 190
- 191
- 192
- 193
- 194
- 195
- 196
- 197
- 198
- 199
- 200
- 201
- 202
- Non-conjugate approach. CTCs from literature are used, which have been determined analytically or (semi-)empirically (i.e. by experimental or numerical studies) as a correlation with the air speed, generally for simplified configurations such as flat plates. Often, the focus of such CTC research is rather on CHTCs, where the CHTCs are still often determined from the heat and mass transfer analogy. An overview of CHTC predictions for flat plates by wind-tunnel experiments is given by Palyvos (2008), within the context of solar collector research. Defraeye et al. (2011a) provided an overview of CHTC predictions for bluff bodies immersed in turbulent boundary layers (e.g. buildings). Although these CTCs account for the influence of the air-flow field to some extent, for example by correlation with the air speed or by including a spatial variation over the surface, there will always exist (often significant) dissimilarities with the specific flow problem of interest, with respect to the flow and scalar fields (geometry, boundary conditions, ...), because actual aerodynamic problems, such as wind flow around buildings and in urban areas, are generally very complex (e.g. Blocken and Carmeliet, 2004; van Hooff and Blocken, 2010; Gousseau et al., 2011). Thereby, the use of such CTCs is considered to be a non-conjugate approach.
 - Semi-conjugate approach. The air-side heat and mass transport for the specific flow problem under study is accounted for by applying case-related CTCs, which can be done in several ways:
 - By including a case-specific spatial variation of the CTCs over the porous surface, which is determined a-priori by a separate flow field calculation (e.g. Kaya et al., 2006). These CTCs can be obtained by solving the flow analytically, i.e. solving boundary-layer equations, or solving the flow numerically, i.e. solving the Navier-Stokes equations (by computational fluid dynamics, CFD). Since the specific flow, thermal and concentration fields are not solved in a transient manner, this approach is considered to be semi-conjugate.
 - By including a temporal variation of the CTCs, namely a dependency of CTCs on the moisture content at the surface (Chen and Pei, 1989). Although the specific flow, thermal and concentration fields are not solved explicitly in this case, they are to some extent related to the transient heat and mass transport at the surface, by which this approach is also considered to be semi-conjugate.
 - Conjugate approach. The heat and mass transport in the air and in the porous material are solved simultaneously in a transient way, i.e. the flow field is solved using boundary-layer equations or Navier-Stokes equations. Continuity of heat and mass fluxes and temperature and mass fractions (e.g. water vapour) at every location on the interface is thus required. Thereby the need for using CTCs is avoided, but instead they can be determined a-posteriori from the conjugate calculation. As such, the spatial and temporal variability of heat and mass transfer in both air flow and porous material can be fully taken into account, and the spatial and temporal variability of the CTCs can be identified. Note that some conjugate models solve air flow assuming a quasi steady-state flow field, based on the assumption that time scales for convection in the air are much smaller than those for heat and mass transfer in the porous material. Thereby, only heat and mass transfer in the air is solved in a transient way (not momentum transfer), which is however only valid for non-buoyant flows since for buoyant flows the flow field also varies in time, as heat acts as an active scalar.

203 Most numerical research on transport in porous materials was devoted to non-conjugate modelling, i.e. by using
204 simplified CTCs, as the focus was rather on the aforementioned porous-material modelling approaches (EPDM:
205 Steeman et al., 2009a; shrinking core models: Hashimoto et al., 2003; macroscopic models: Ben Nasrallah and Perre,

206 1988; Ilic and Turner, 1989; Turner and Ilic, 1990; Prat, 1991; Kallel et al., 1993; Boukadida and Ben Nasrallah, 1995;
207 Zhang et al., 1999; Boukadida et al., 2000; Nijdam et al., 2000; Haghi, 2001; Lu et al., 2005; Kocaefe et al., 2006;
208 Younsi et al., 2006; Janssen et al., 2007; Alexandri and Jones, 2007; Lu and Shen, 2007; Murugesan et al., 2008; pore-
209 network models: Laurindo and Prat, 1996; Laurindo and Prat, 1998; Le Bray and Prat, 1999; Yiotis et al., 2001; Plourde
210 and Prat, 2003; Yiotis et al., 2005; Yiotis et al., 2006; Prat, 2007; Surasani et al., 2008).

211
212 Numerical models which apply a conjugate or semi-conjugate approach are much scarcer. An overview of the available
213 models for convective heat and mass transfer applications with water as the mass transfer component, to the current
214 knowledge of the authors, is given in Table 1. For drying applications, only conjugate models for convective drying are
215 considered, e.g. no microwave drying. In addition, water is considered to be only in the liquid or gas state, thus freeze
216 drying (e.g. Nam and Song, 2007) is also not included. Note that, apart from applications for moisture transport, such a
217 conjugate approach has also been applied for VOC transfer for indoor environments (e.g. Yang et al., 2001) and for
218 building energy simulation programs (Chen and Srebric, 2000; Zhai et al., 2002; Mora et al., 2003; Zhai and Chen,
219 2004; Zhai, 2006), where air-flow modelling (e.g. with CFD) is used to provide more accurate thermal boundary
220 conditions for the interior and exterior of the building envelope. CFD was already often applied for such convective
221 transfer predictions in the past (e.g. Karava et al., 2011; Defraeye et al., 2012). The following remarks can be made
222 regarding the (semi-)conjugate models presented in Table 1:

- 223 • Conjugate modelling is a relatively recent development, as the majority of the progress has been made during
224 the past decade.
- 225 • Mainly 2D conjugate modelling has been performed.
- 226 • Although these (semi-)conjugate models were mainly developed for drying applications, this does not
227 necessarily imply that the material is fully saturated.
- 228 • Radiation is usually not accounted for in these models.
- 229 • Validation of these conjugate models is often not performed. When performed, experimental data from other
230 researchers is often used, and the transport in the porous material and in the air is usually validated separately.

231
232 Often, the reason for applying non-conjugate modelling instead of the (semi-)conjugate approach is the additional
233 modelling effort that has to be performed: (1) The air-flow domain also has to be solved, which inherently implies an
234 increased computational cost; (2) As (semi-)conjugate models are not yet commercially available, they consist of in-
235 house developed codes in which an air-flow model has been programmed or where a coupling procedure with an
236 existing air-flow model (e.g. CFD software) was established. A more detailed evaluation of the convective exchange
237 processes by means of a conjugate approach has shown to enhance the numerical predictive accuracy, e.g. for
238 convective drying processes (e.g. Erriguible et al., 2006; Defraeye et al., 2012). However, as discussed above, the
239 impact of the imposed convective boundary conditions on the heat and mass transfer from the porous material is not
240 always significant, by which non-conjugate modelling is sufficiently accurate for certain applications. The necessity of
241 accurate convective transfer modelling is illustrated in the next section by two numerical case studies.

242

243 **3. Relevance of accurate surface convective transfer predictions**

244 **3.1. Background**

245 Before describing both case studies, the general characteristics of convective heat and mass exchange of porous
246 materials with external air flow are briefly discussed. This discussion is written from the perspective of quasi-saturated
247 porous materials, thus for drying processes, due to their relevance for many industrial applications (Mujumdar, 2006).
248 Here, water is considered as the mass transfer component.

249
250 A typical drying process is depicted in Figure 1, with respect to mass flow rate ($g_{v,w}$), surface temperature (T_w) and
251 relative humidity at the surface (RH_w). After an initial transition period (TP), the material experiences the constant
252 drying rate period (CDRP), given that the air-material interface remains wet. The CDRP is characterised by a relative
253 humidity (RH) of quasi 100% at the surface, a constant drying rate and a constant material temperature, which is equal
254 to the wet bulb temperature (T_{wb}) if no radiative heat flows at the surface and (conductive) heat flows from the interior
255 of the porous material are present. In this case, the convective heat supply to the interface is quasi entirely used for the
256 evaporation of water, which requires latent heat for the phase change from liquid water to vapour.

257
258 As evaporation occurs at the air-porous material interface during the CDRP, the drying rate is determined by the air-
259 flow conditions and not by the porous-material transport properties. Nevertheless, the porous-material transport
260 properties do affect the length of the CDRP, since it is dependent on the supply of liquid to the surface. When the
261 material dries out at the interface, the decreasing drying rate period (DDRP) sets in, which is characterised by a lower
262 drying rate (see Figure 1). During DDRP, the liquid water front recedes from the surface and water, once evaporated,
263 must diffuse out via the “dry” outer porous material layer. This dry layer can be seen as an additional resistance to
264 liquid water transport from the inside of the material. Due to this material resistance, in addition to the boundary-layer
265 resistance, the drying rate of most porous materials during the DDRP is thereby much less sensitive to the convective
266 boundary conditions. This decrease in drying rate is accompanied by a temperature increase since less latent heat is
267 required for the evaporation of water. Also for applications where materials do not contain any liquid water thus where
268 only vapour transport occurs, the convective moisture exchange rate with the environment is usually dominated by the
269 vapour diffusion in the material, rather than by the air-flow field. Note however that the sensitivity of the drying process
270 to convective heat transfer can be pronounced during the DDRP in some cases, as discussed in section 4.

271
272 Although the insensitivity of mass transfer from porous materials to the convective boundary conditions during the
273 DDRP is generally known (Mujumdar, 2006), it is often left unacknowledged resulting in too detailed modelling of the
274 convective conditions. For indoor climate analysis for example, high spatial resolution CTCs are often determined as a
275 function of different ventilation system characteristics by means of CFD, although these CTCs are usually not
276 dominating the moisture transport kinetics. Here, accurate and detailed CTCs are actually not essential for the resulting
277 modelling accuracy. In the next section, two case studies illustrate the impact and relevance of convective transfer
278 predictions for numerical modelling of convective heat and mass exchange processes.

279 280 **3.2. Case studies**

281 **3.2.1. Configuration**

282 The setup used in both case studies is taken from the study of James et al. (2010). They analysed the hygroscopic
283 buffering of gypsum boards experimentally by means of a small closed-circuit wind-tunnel setup and made a
284 comparison with numerical simulations. The same configuration was also used by Defraeye et al. (2012) to investigate
285 convective drying of a mineral plaster plate numerically. In these studies, a two-dimensional fully-developed laminar

286 channel flow (channel height $H = 20.5$ mm) is produced over the porous material (length $L_{PM} = 500$ mm and thickness
287 $D_{PM} = 37.5$ mm, i.e. 3 gypsum boards of 12.5 mm or a mineral plaster plate of 37.5 mm), which is mounted flush with
288 one of the channel walls. The porous material is insulated (adiabatic conditions) and made impermeable for moisture on
289 its remaining surfaces. This experimental setup is described in detail by Talukdar et al. (2007).

290

291 In the present numerical study, this configuration is evaluated for two cases: (1) case 1: the experiment of James et al.
292 (2010), which involves hygroscopic loading of gypsum boards; (2) case 2: the numerical study of Defraeye et al.
293 (2012), which involves convective drying of a capillary saturated mineral plaster plate. In the second case, the only
294 differences with the experiment of James et al. (2010) are the used porous material (mineral plaster) and the initial
295 porous-material moisture content and temperature.

296

297 **3.2.2. Computational model**

298 The computational model used for the numerical analyses is presented in Figure 2, together with the imposed boundary
299 conditions for both cases. A detailed description of this computational model is given in Defraeye et al. (2012) and is
300 not repeated here. The computational model, its boundary conditions and the material properties are in accordance with
301 the experiment of James et al. (2010) for both cases, except for the porous material type and its initial moisture content
302 and temperature of case 2. For case 1, the gypsum board is initially conditioned at 30% RH and 23.3°C. For case 2, the
303 mineral plaster is assumed to be initially unsaturated, but at capillary saturation moisture content (126 kg/m^3) at a
304 temperature of 20.0°C. This temperature is approximately equal to the wet bulb temperature ($\approx 20^\circ\text{C}$ for $T_{ref} = 23.8^\circ\text{C}$
305 and $RH_{ref} = 71.9\%$ RH). The material properties for the plaster are given in Defraeye et al. (2012); those of gypsum
306 board are given in James et al. (2010). Gypsum board is actually a layered composite material consisting of gypsum and
307 paper liner. In this study, gypsum board is modelled as a single material, in accordance with James et al. (2010), which
308 determined the relevant material properties accordingly.

309

310 **3.2.3. Numerical simulation**

311 Conjugate modelling implies that both the transport in the air and in the porous material are solved. The air-flow
312 simulations are performed assuming laminar flow, due to the low Reynolds numbers ($Re = 1100$, see Figure 2), with the
313 commercial computational fluid dynamics (CFD) code Fluent 6.3 (Fluent, 2006), which uses the control volume
314 method. Radiation between the channel walls is not considered because: (1) for case 1, the experiment is nearly
315 isothermal, by which the influence of radiation is quasi negligible; (2) for case 2, the focus of Defraeye et al. (2012) was
316 also on the validity of the heat and mass transfer analogy, which cannot be valid if radiation is taken into account. Note
317 that James et al. (2010) also did not account for radiation and that they used a CHTC which was determined from the
318 CMTC by means of the heat and mass transfer analogy (from Iskra and Simonson, 2007). The porous-material
319 simulations are performed with a non-commercial finite-element porous-material model (or heat-air-moisture (HAM)
320 transport model), called HAMFEM. Detailed numerical modelling information can be found in Janssen et al. (2007).
321 Since two different programs are used for air-flow and porous-material modelling (Fluent 6.3 and HAMFEM), an
322 external coupling protocol between these programs was implemented, where the exchange of boundary conditions
323 between the two programs is performed once every time step. More details on this conjugate model can be found in
324 Defraeye et al. (2012).

325

326 In addition, the conjugate modelling approach is compared with porous-material modelling (with HAMFEM) using
327 spatially and temporally constant CTCs, which will be referred to as the constant CTC approach. The applied CTCs for
328 this approach are specified for each case in sections 3.2.4 and 3.2.5.

329

330 **3.2.4. Case 1: Hygroscopic loading of gypsum boards**

331 For a typical hygroscopic loading experiment, the moisture content of a material, achieved at equilibrium with air at a
332 set relative humidity, changes due to exposure to air with a different relative humidity. Hygroscopic loading usually
333 involves only vapour transport, and no liquid transport. Thereby, the material can actually be considered to be in a
334 relatively late state of the DDRP. A nearly isothermal experiment was used by James et al. (2010) to validate different
335 porous-material models (including the porous-material model used in the proposed conjugate model) for hygroscopic
336 loading of 3 gypsum boards, using the wind-tunnel setup described in section 3.2.1. Here, both relative humidity and
337 temperature were measured in between two gypsum boards (using capacitive humidity sensors and thermocouples,
338 respectively), together with the moisture accumulation of the ensemble of boards (using load cells). The conjugate
339 simulation results are compared with the experimental data of James et al. (2010) in Figure 3. Here, the temperature and
340 relative humidity in the middle of the material below the first gypsum board are shown ($x = 250$ mm, $y = -12.5$ mm, see
341 Figure 2) as well as the total moisture accumulation in the material. In addition, the results of the constant CTC
342 approach are also included. Here, the spatially and temporally constant CTCs, as determined experimentally by James et
343 al. (2010), were imposed ($\text{CHTC} = 3.45$ W/m²K, $\text{CMTC} = 2.41 \times 10^{-8}$ s/m). Both the conjugate model and the constant
344 CTC approach seem to predict the relative humidity, temperature and moisture accumulation quite well, i.e.
345 approximately within the experimental uncertainty, and produce very similar results, indicating that no significantly
346 increased accuracy is obtained with the conjugate model.

347

348 The good agreement between the porous-material model using constant CTCs and the conjugate model is due to the
349 very small sensitivity of the heat and mass transport to the flow field (James et al., 2010). It was shown by Defraeye et
350 al. (2012) (see also section 3.2.5) however that the (surface-averaged) CTCs used in both approaches actually differed
351 significantly ($\approx 50\%$) for this flat-plate configuration. This low sensitivity to convective vapour transfer originates from
352 the relatively high resistance of gypsum board to vapour transfer (R_{GB}), compared to that of the boundary layer (R_{BL}).
353 These resistances are compared in Figure 4 as a function of the thickness of the gypsum board (D_{GB}) for different RH of
354 the gypsum board. Here, $R_{\text{BL}} = \text{CMTC}^{-1}$ and $R_{\text{GB}} = D_{\text{GB}}/\delta_{\text{v,GB}}$, where $\delta_{\text{v,GB}}$ is the water vapour diffusion coefficient of
355 gypsum board. R_{BL} quickly becomes much smaller than R_{GB} with increasing D_{GB} . As a result, for many porous
356 materials, the vapour uptake/release kinetics are mainly determined by the material itself and not by the air flow,
357 resulting in a good agreement between conjugate and constant CTC approaches. Actually, the discrepancies with
358 experiments were found to result mainly from experimental uncertainties on the material properties which are used in
359 the porous-material model (James et al., 2010). For these types of problems, where the largest resistances to moisture
360 transfer are located in the porous material (equivalent to the DDRP), (semi-)conjugate modelling clearly does not
361 contribute significantly to an increased modelling accuracy.

362

363 **3.2.5. Case 2: Convective drying of a mineral plaster plate**

364 For convective drying of a capillary saturated porous flat plate (mineral plaster), Defraeye et al. (2012) compared
365 porous-material modelling using constant (spatial and temporal) CTCs with conjugate modelling. The CTCs used by the
366 constant CTC approach were obtained from surface-averaged CHTC values from CFD simulations, combined with the

367 analogy to determine the CMTC ($CHTC = 5.34 \text{ W/m}^2\text{K}$, $CMTC = 3.77 \times 10^{-8} \text{ s/m}$). The drying rate, surface temperature
368 and relative humidity at the surface of the two approaches are shown as a function of dimensionless time in Figure 5.
369 Due to their spatial variability for the conjugate approach, these parameters are presented at specific locations on the
370 porous-material surface, namely at $x = 0, 0.25$ and 0.5 m , but the surface-averaged $g_{v,w}$ is also presented. The drying
371 rates are scaled with the drying rate during the CDRP from the constant CTC approach ($g_{v,w,CDRP}$).

372
373 For the constant CTC approach, the CDRP and DDRP (see Figure 1) can clearly be distinguished. For the conjugate
374 approach, the surface-averaged drying rate shows a much shorter CDRP, which is found to be related to the two-
375 dimensional drying effect: the surface near the leading edge dries out first and quickly, by which the total drying rate
376 quickly decreases, while the remaining part of the surface dries out later. A CDRP can be distinguished at specific
377 locations on the surface, where its duration increases with distance from the leading edge. Distinct peaks in the drying
378 rate appear, which approximately correspond with the moment in time where the surface dries out locally ($RH < 100\%$,
379 see Figure 5c). These peaks result from the downstream progression of the drying front with time (see Defraeye et al.,
380 2012), where the drying front indicates the separation between the dried-out and still-wet part of the interface. When
381 considering the surface-averaged drying rates of both approaches in Figure 5a, the sensitivity to the convective
382 boundary conditions is clearly less pronounced during the DDRP, due to the additional material resistance.

383
384 As the conjugate approach does not require CTCs to represent the convective boundary conditions, it allows calculating
385 the CTCs a-posteriori, by which their temporal and spatial variability can be identified. The resulting CMTCs are shown
386 in Figure 6 as a function of dimensionless time and location on the interface by means of a contour plot. A distinct
387 spatial variation can be noticed, with higher values closer to the leading edge. In addition, a strong temporal variability
388 can be noticed, especially at the transition from CDRP to DDRP, i.e. when the surface locally dries out. The temporal
389 variation indicates that CTCs are not only intrinsically related to the specific flow field, which is responsible for the
390 spatial CTC variation, but that they are also dependent on the transient temperature and moisture distribution in the flow
391 field (boundary layer) and at the air-porous material interface.

392

393 **4. Discussion**

394 An alternative to porous-material modelling using constant (spatial and/or temporal) CTCs has become more popular in
395 the past decades, namely conjugate modelling. Conjugate modelling allows accounting for spatial and temporal
396 variations in convective boundary conditions and thereby it circumvents the use of CTCs, which actually quantify the
397 air-side heat and mass transfer in a rather simplified way. As shown in section 3, the need for detailed modelling of
398 convective boundary conditions is however strongly dependent on the moisture transport characteristics of the porous
399 material. In general, conjugate modelling will improve simulation accuracy during the CDRP and the transition to the
400 DDRP, i.e. when the surface is (partially) wet, since then the air flow mainly determines the drying rate. During the
401 DDRP however, the impact of the CTC predictions on the accuracy of exchange processes was shown to be more
402 limited (section 3.2.4), as the internal vapour resistance of the porous material dictates the liquid water removal rate
403 from the material, and (semi-)conjugate modelling does not seem to be required. Instead of accurate modelling of the
404 convective boundary conditions, material characterisation related to liquid and vapour transport is more critical here.

405

406 However, convective heat transfer can play a significant role throughout the entire drying process (also during the
407 DDRP) due to its impact on the convective moisture exchange of the porous material with the environment, particularly

408 for strong non-isothermal problems. The reasons for this are that: (1) convective heat exchange determines, in part, the
409 latent heat supply required for moisture removal from the porous material; (2) the boundary-layer resistance for heat
410 transfer often lies much closer to the heat transfer resistance of typical porous materials, by which the sensitivity to
411 convective heat transfer becomes larger; (3) mass transfer in porous materials can be thermally driven. Although highly
412 accurate convective mass transfer predictions are not required during the DDRP, and probably in any hygroscopic
413 loading case, conjugate modelling of convective heat (not mass) transfer could have a pronounced effect on the
414 predicted heat and mass exchange. The impact of the convective heat flow component on drying processes will however
415 be strongly case dependent, as it is a result from the specific heat balance at the surface, which includes radiation
416 amongst others. Therefore it is difficult to state general conclusions in this matter. Such an assessment however
417 inherently requires conjugate modelling, and the suggestion of guidelines for such an assessment is a topic of future
418 research.

419
420 When evaluating a conjugate heat and mass exchange problem numerically, it is thus advised to evaluate a-priori the
421 sensitivity of the exchange processes to the convective boundary conditions, e.g. by comparing boundary-layer and
422 material resistances. From this analysis, the required degree of detail for the specification of the convective boundary
423 conditions can be determined. In some studies, conjugate modelling is required but is not applied because a conjugate
424 model is not available or in order to limit the computational expense. In this case, it is strongly suggested to account for
425 the spatial variation of the CTCs when performing porous-material modelling, for example by determining the CHTC
426 by means of a CFD study and the corresponding CMTC using the analogy. Furthermore, for flow configurations which
427 have a more applied nature than the ones presented in this paper, e.g. in actual industrial driers, flow fields and
428 exchange processes will be more complex due to the presence of strong radiation, buoyancy, turbulence, etc. Here, the
429 increased accuracy from conjugate modelling will often be even more pronounced. Turbulence, for example, will
430 usually enhance transfer rates compared to laminar flow, but is highly dependent on the specific flow field, flow
431 configuration and flow history. Thereby, the resulting ensemble of turbulence structures (eddies) is very case specific,
432 i.e. unique. This case specific nature of turbulent flow, and thus of turbulent convective transfer (CTCs), hence
433 increases the need for a conjugate assessment of (convective) heat and mass transfer from porous materials, compared
434 to laminar flow.

435
436 Another significant advantage of the conjugate modelling approach, often left unacknowledged, is that it does not rely
437 on the heat and mass transfer analogy. As this analogy is only valid under strict conditions (see Defraeye et al., 2012),
438 no radiation amongst others, it cannot be used in principle for the majority of the conjugate problems in engineering,
439 such as drying (Chen et al., 2002). However, it is applied regularly and it is often found to be sufficiently accurate. On
440 the other hand, conjugate modelling is an appropriate tool to investigate the validity of the analogy under different
441 conditions.

442
443 Finally, conjugate models (and related required software) are not yet widely known or used, due to their limited
444 (commercial) availability amongst others. Thereby, the conjugate studies performed up to now considered simplified
445 configurations (see Table 1) using in-house developed codes or coupling between/with existing codes. In this stage of
446 active model development, validation of such conjugate models with detailed experiments is imperative. Such
447 experiments are however very scarce (e.g. Belhamri and Fohr, 1996) and are still an active topic of ongoing research
448 (Murugesan et al., 2001). Preferably, future experiments should be specifically designed for conjugate model validation:

449 as shown in section 3.2.4, some experiments do not have a large sensitivity to convective exchange, by which they are
450 not appropriate because they mainly validate the porous-material model.

451

452 **5. Conclusions**

453 In this study, an overview was given of existing methods to model convective heat and mass transfer at air-porous
454 material interfaces for porous-material modelling purposes. Instead of using well-established convective transfer
455 coefficients (CTCs), conjugate modelling is clearly becoming a more widely used, and inherently more accurate,
456 approach. Based on two case studies, namely hygroscopic loading and convective drying, the improved accuracy of this
457 approach was indicated. Conjugate modelling has the advantage that it does not require CTCs, but it can identify them
458 a-posteriori. As shown in this study, a large spatial and temporal CTC variability can be found. Furthermore, the use of
459 the heat and mass transfer analogy is not required. These advantages are especially relevant for complex flow problems,
460 such as in industrial drier systems. However, the sensitivity to the convective boundary conditions can be limited in
461 some cases, e.g. during the DDRP. Instead of significantly improving the accuracy here, conjugate modelling will rather
462 impose an additional modelling effort, which sometimes even requires conjugate model code development as these
463 models are not readily (commercially) available. In such cases, the focus should rather be on ensuring the accuracy of
464 porous-material modelling. Before embarking on a conjugate modelling study, which often implies CFD modelling, it is
465 therefore advised to perform a-priori a sensitivity analysis with respect to the convective boundary conditions. In some
466 cases, sufficient accuracy can be obtained using empirical CTCs from literature.

467

468 **Acknowledgements**

469 Thijs Defraeye is a postdoctoral fellow of the Research Foundation – Flanders (FWO) and acknowledges its support.
470 Financial support by the Research Foundation – Flanders (project FWO G.0603.08) and K.U.Leuven (project OT
471 08/023) is also gratefully acknowledged. These sponsors had no involvement in: the study design, in the collection,
472 analysis and interpretation of data; in the writing of the manuscript; and in the decision to submit the manuscript for
473 publication.

474

475 **References**

- 476 Alexandri, E., Jones, P., 2007. Developing a one-dimensional heat and mass transfer algorithm for describing the effect
477 of green roofs on the built environment: Comparison with experimental results. *Building and Environment* 42 (8),
478 2835-2849.
- 479 Belhamri, A., Fohr, J.P., 1996. Heat and mass transfer along a wetted porous plate in an airstream. *AIChE Journal* 42
480 (7), 1833-1843.
- 481 Ben Nasrallah, S., Perre, P., 1988. Detailed study of a model of heat and mass transfer during convective drying of
482 porous media. *International Journal of Heat and Mass Transfer* 31 (5), 957-967.
- 483 Blocken, B., Carmeliet, J., 2004. A review of wind-driven rain research in building science. *Journal of Wind
484 Engineering and Industrial Aerodynamics* 92 (13), 1079-1130.
- 485 Blocken, B., Roels, S., Carmeliet, J., 2007. A combined CFD-HAM approach for wind-driven rain on building facades.
486 *Journal of Wind Engineering and Industrial Aerodynamics* 95 (7), 585-607.
- 487 Blocken, B., Defraeye, T., Derome, D., Carmeliet, J., 2009. High-resolution CFD simulations of forced convective heat
488 transfer coefficients at the facade of a low-rise building. *Building and Environment* 44 (12), 2396-2412.

- 489 Blunt, M.J., 2001. Flow in porous media - pore-network models and multiphase flow. *Current Opinion in Colloid &*
490 *Interface Science* 6 (3), 197-207.
- 491 Boukadida, N., Ben Nasrallah, S., 1995. Two dimensional heat and mass transfer during convective drying of porous
492 media. *Drying Technology* 13 (3), 661-694.
- 493 Boukadida, N., Ben Nasrallah, S., Perre, P., 2000. Mechanism of two-dimensional heat and mass transfer during
494 convective drying of porous media under different drying conditions. *Drying Technology* 18 (7), 1367-1388.
- 495 Bowen, R.M, 1980. Incompressible porous media models by use of the theory of mixtures. *International Journal of*
496 *Engineering Science* 18 (9), 1129-1148.
- 497 Carmeliet, J., Blocken, B., Defraeye, T., Derome, D., 2011. Moisture phenomena in whole building performance
498 prediction, in: Hensen, J.L.M., Lamberts, R. (Eds.), *Building Performance Simulation for Design and Operation*.
499 Taylor and Francis, London, UK.
- 500 Carmeliet, J., Descamps, F., Houvenaghel, G., 1999. A multiscale network model for simulating moisture transfer
501 properties of porous media. *Transport in Porous Media* 35, 67-88.
- 502 Chandra Mohan, V.P., Talukdar, P., 2010. Three dimensional numerical modeling of simultaneous heat and moisture
503 transfer in a moist object subjected to convective drying. *International Journal of Heat and Mass Transfer* 53 (21-
504 22), 4638-4650.
- 505 Chen, P., Pei, D.C.T., 1989. A mathematical model of drying processes. *International Journal of Heat and Mass*
506 *Transfer* 32 (2), 297-310.
- 507 Chen, Q., Srebric, J., 2000. Application of CFD tools for indoor and outdoor environment design. *International Journal*
508 *on Architectural Science* 1 (1), 14-29.
- 509 Chen, X.D., Lin, S.X.Q., Chen, G., 2002. On the ratio of heat and mass transfer coefficient for water evaporation and its
510 impact upon drying modelling. *International Journal of Heat and Mass Transfer* 45 (21), 4369-4372.
- 511 Chilton, T.H., Colburn, A.P., 1934. Mass transfer (absorption) coefficients. *Industrial and Engineering Chemistry* 26
512 (11), 1183-1187.
- 513 Cloutier, A., Fortin, Y., Dhatt, G., 1992. A wood drying finite element model based on the water potential concept.
514 *Drying technology* 10 (5), 1151-1181.
- 515 Cunningham, M.J., 1992. Effective penetration depth and effective resistance in moisture transfer. *Building and*
516 *Environment* 27 (3), 379-386.
- 517 De Bonis, M.V., Ruocco, G., 2008. A generalized conjugate model for forced convection drying based on an
518 evaporative kinetics. *Journal of Food Engineering* 89 (2), 232-240.
- 519 Defraeye, T., Blocken, B., Carmeliet, J., 2010. CFD analysis of convective heat transfer at the surfaces of a cube
520 immersed in a turbulent boundary layer. *International Journal of Heat and Mass Transfer* 53 (1-3), 297-308.
- 521 Defraeye, T., Blocken, B., Carmeliet, J., 2011a. Convective heat transfer coefficients for exterior building surfaces:
522 Existing correlations and CFD modelling. *Energy Conversion and Management* 52 (1), 512-522.
- 523 Defraeye, T., Blocken, B., Carmeliet, J., 2011b. An adjusted temperature wall function for turbulent forced convective
524 heat transfer for bluff bodies in the atmospheric boundary layer. *Building and Environment* 46 (11), 2130-2141.
- 525 Defraeye, T., Blocken, B., Carmeliet, J., 2012. Analysis of convective heat and mass transfer coefficients for convective
526 drying of a porous flat plate by conjugate modelling. *International Journal of Heat and Mass Transfer* 55 (1-3), 112-
527 124.
- 528 Dolinskiy, A.A., Dorfman, A.S.H., Davydenko, B.V., 1991. Conjugate heat and mass transfer in continuous processes
529 of convective drying. *International Journal of Heat and Mass Transfer* 34 (11), 2883-2889.

Defraeye T., Blocken B., Derome D., Nicolai B., Carmeliet J., (2012), Convective heat and mass transfer modelling at air-porous material interfaces: overview of existing methods and relevance, *Chemical Engineering Science* 74, 49-58. <http://dx.doi.org/10.1016/j.ces.2012.02.032>

- 530 Erriguible, A., Bernada, P., Couture, F., Roques, M., 2005. Modeling of heat and mass transfer at the boundary between
531 a porous medium and its surroundings. *Drying Technology* 23 (3), 455-472.
- 532 Erriguible, A., Bernada, P., Couture, F., Roques, M., 2006. Simulation of convective drying of a porous medium with
533 boundary conditions provided by CFD. *Chemical Engineering Research and Design* 84 (2), 113-123.
- 534 Gousseau, P., Blocken, B., Stathopoulos, T., van Heijst, G.J.F., 2011. CFD simulation of near-field pollutant dispersion
535 on a high-resolution grid: a case study by LES and RANS for a building group in downtown Montreal. *Atmospheric*
536 *Environment* 45 (2), 428-438.
- 537 Fluent Inc., *Fluent 6.3 User's Guide*, Lebanon - New Hampshire, USA, 2006.
- 538 Haghi, A.K., 2001. A mathematical model of the drying process. *Acta Polytechnica* 41 (3), 20-23.
- 539 Hashimoto, A., Stenström, S., Kameoka, T., 2003. Simulation of convective drying of wet porous materials. *Drying*
540 *Technology* 21 (8), 1411-1431.
- 541 Hoang, M., Verboven, P., Baelmans, M., Nicolai, B., 2003. A continuum model for airflow, heat and mass transfer in
542 bulk of chicory roots. *Transactions of the ASAE* 46 (6), 1603-1611.
- 543 Hoang, M., Verboven, P., De Baerdemaeker, J., Nicolai, B., 2000. Analysis of the air flow in a cold store by means of
544 computational fluid dynamics. *International Journal of Refrigeration* 23 (2), 127-140.
- 545 Ilic, M., Turner, I.W., 1989. Convective drying of a consolidated slab of wet porous material. *International Journal of*
546 *Heat and Mass Transfer* 32 (12), 2351-2362.
- 547 Iskra, C.R., James, C., Talukdar, P., Simonson, C.J., 2009. Convective mass transfer coefficients for gypsum and wood
548 panelling. *Journal of ASTM International* 6 (4), 1-18.
- 549 Iskra, C.R., Simonson, C.J., 2007. Convective mass transfer coefficient for a hydrodynamically developed airflow in a
550 short rectangular duct. *International Journal of Heat and Mass Transfer* 50 (11-12), 2376-2393.
- 551 James, C., Simonson, C.J., Talukdar, P., Roels, S., 2010. Numerical and experimental data set for benchmarking
552 hygroscopic buffering models. *International Journal of Heat and Mass Transfer* 53 (19-20), 3638-3654.
- 553 Janssen, H., Blocken, B., Carmeliet, J., 2007. Conservative modelling of the moisture and heat transfer in building
554 components under atmospheric excitation. *International Journal of Heat and Mass Transfer* 50 (5-6), 1128-1140.
- 555 Kallel, F., Galanis, N., Perrin, B., Javelas, R., 1993. Effects of moisture on temperature during drying of consolidated
556 porous materials. *Transactions of the ASME: Journal of Heat Transfer* 115, 724-733.
- 557 Karava, P., Jubayer, C.M., Savory, E., 2011. Numerical modelling of forced convective heat transfer from the inclined
558 windward roof of an isolated low-rise building with application to photovoltaic/thermal systems. *Applied Thermal*
559 *Engineering* 31 (11-12), 1950-1963.
- 560 Kaya, A., Aydin, O., Dincer, I., 2006. Numerical modeling of heat and mass transfer during forced convection drying of
561 rectangular moist objects. *International Journal of Heat and Mass Transfer* 49 (17-18), 3094-3103.
- 562 Kocaefe, D., Younsi, R., Chaudry, B., Kocaefe, Y., 2006. Modeling of heat and mass transfer during high temperature
563 treatment of aspen. *Wood Science and Technology* 40 (5), 371-391.
- 564 Kowalski, S.J., 2010. Control of mechanical processes in drying. Theory and experiment. *Chemical Engineering*
565 *Science* 65 (2), 890-899.
- 566 Kowalski, S.J., Pawlowski, A., 2011. Intermittent drying of initially saturated porous materials. *Chemical Engineering*
567 *Science* 66 (9), 1893-1905.
- 568 Lamnatou, Chr., Papanicolaou, E., Belessiotis, V., Kyriakis, N., 2009. Conjugate heat and mass transfer from a drying
569 rectangular cylinder in confined air flow. *Numerical Heat Transfer, Part A: Applications* 56 (5), 379-405.

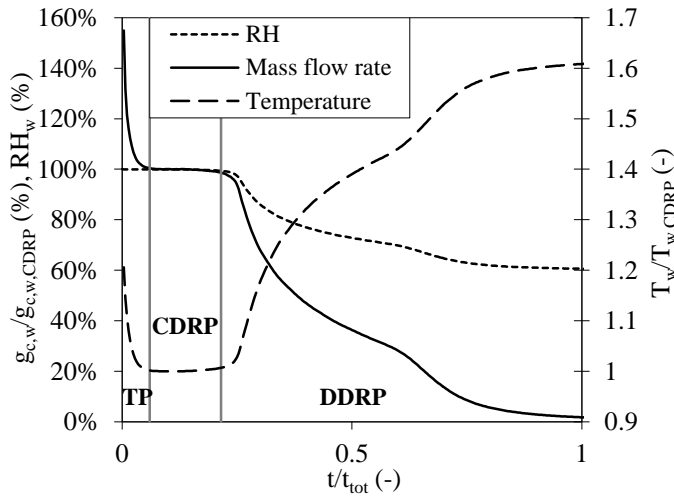
Defraeye T., Blocken B., Derome D., Nicolai B., Carmeliet J., (2012), Convective heat and mass transfer modelling at air-porous material interfaces: overview of existing methods and relevance, *Chemical Engineering Science* 74, 49-58. <http://dx.doi.org/10.1016/j.ces.2012.02.032>

- 570 Lamnatou, Chr., Papanicolaou, E., Belessiotis, V., Kyriakis, N., 2010. Finite-volume modelling of heat and mass
571 transfer during convective drying of porous bodies - Non-conjugate and conjugate formulations involving the
572 aerodynamic effects. *Renewable Energy* 35 (7), 1391-1402.
- 573 Laurindo, J.B., Prat, M., 1996. Numerical and experimental network study of evaporation in capillary porous media.
574 Phase distributions. *Chemical Engineering Science* 51 (23), 5171-5185.
- 575 Laurindo, J.B., Prat, M., 1998. Numerical and experimental network study of evaporation in capillary porous media.
576 Drying rates. *Chemical Engineering Science* 53 (12), 2257-2269.
- 577 Le Bray, Y., Prat, M., 1999. Three-dimensional pore network simulation of drying in capillary porous media.
578 *International Journal of Heat and Mass Transfer* 42 (22), 4207-4224.
- 579 Lu, T., Jiang, P., Shen, S., 2005. Numerical and experimental investigation of convective drying in unsaturated porous
580 media with bound water. *Heat and Mass Transfer* 41 (12), 1103-1111.
- 581 Lu, T., Shen, S.Q., 2007. Numerical and experimental investigation of paper drying: Heat and mass transfer with phase
582 change in porous media. *Applied Thermal Engineering* 27 (8-9), 1248-1258.
- 583 Luikov, A.V., 1966. *Heat and Mass Transfer in Capillary-Porous Bodies*, first ed. Pergamon Press, New York, USA.
- 584 Luikov, A.V., 1975. Systems of differential equations of heat and mass transfer in capillary-porous bodies. *International*
585 *Journal of Heat and Mass Transfer* 18 (1), 1-14.
- 586 Masmoudi, W., Prat, M., 1991. Heat and mass transfer between a porous medium and a parallel external flow.
587 Application to drying of capillary porous materials. *International Journal of Heat and Mass Transfer* 34 (8), 1975-
588 1989.
- 589 Moonen, P., Sluys, L.J., Carmeliet, J., 2010. A continuous-discontinuous approach to simulate physical degradation
590 processes in porous media. *International Journal for Numerical Methods in Engineering* 84 (9), 1009-1037.
- 591 Mora, L., Gadgil, A. J., Wurtz, E., 2003. Comparing zonal and CFD model predictions of isothermal indoor airflows to
592 experimental data. *Indoor Air* 13 (2), 77-85.
- 593 Mortensen, L.H., Woloszyn, M., Rode, C., Peuhkuri, R., 2007. Investigation of microclimate by CFD modeling of
594 moisture interactions between air and constructions. *Journal of Building Physics* 30(4), 279-315.
- 595 Mujumdar, A.S. (Editor), 2006. *Handbook of Industrial Drying*, third ed. Taylor & Francis Group, Boca Raton, USA.
- 596 Murugesan, K., Lo, D.C., Young, D.L., Chen, C.W., Fan, C.M., 2008. Convective drying analysis of three-dimensional
597 porous solid by mass lumping finite element technique. *Heat and Mass Transfer* 44 (4), 401-412.
- 598 Murugesan, K., Suresh, H.N., Seetharamu, K.N., Aswatha Narayana, P.A., Sundararajan, T., 2001. A theoretical model
599 of brick drying as a conjugate problem. *International Journal of Heat and Mass Transfer* 44 (21), 4075-4086.
- 600 Nam, J.H., Song, C.S., 2007. Numerical simulation of conjugate heat and mass transfer during multi-dimensional freeze
601 drying of slab-shaped food products. *International Journal of Heat and Mass Transfer* 50 (23-24), 4891-4900.
- 602 Nijdam, J.J., Langrish, T.A.G., Keey, R.B., 2000. A high-temperature drying model for softwood timber. *Chemical*
603 *Engineering Science* 55 (18), 3585-3598.
- 604 Oliveira, L.S., Fortes, M., Haghighi, K., 1994. Conjugate analysis of natural convective drying of biological materials,
605 *Drying Technology* 12 (5), 1167-1190.
- 606 Oliveira, L.S., Haghighi, K., 1998. Conjugate heat and mass transfer in convective drying of porous media. *Numerical*
607 *Heat Transfer, Part A: Applications* 34, 105-117.
- 608 Palyvos, J.A., 2008. A survey of wind convection coefficient correlations for building envelope energy systems'
609 modelling. *Applied Thermal Engineering* 28 (8-9), 801-808.

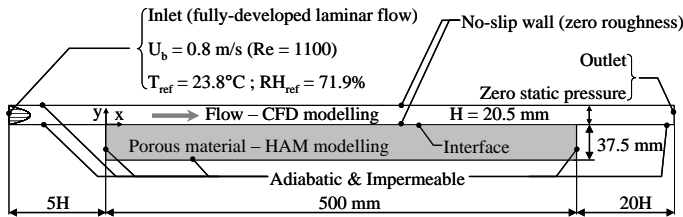
- 610 Philip, J.R., De Vries, D.A., 1957. Moisture movement in porous materials under temperature gradients. Transactions
611 American Geophysical Union 38 (2), 222-232.
- 612 Plourde, F., Prat, M., 2003. Pore network simulations of drying of capillary porous media. Influence of thermal
613 gradients. *International Journal of Heat and Mass Transfer* 46 (7), 1293-1307.
- 614 Poupeleer, A.S., Roels, S., Carmeliet, J., Van Gemert, D., 2006a. Diffusion-convection transport of salt solutions in
615 cracked porous building materials. Part 1: Parameters, model description and application to cracks. *International*
616 *Journal for Restoration of Buildings and Monuments* 12 (3), 187-204.
- 617 Poupeleer, A.S., Roels, S., Carmeliet, J., Van Gemert, D., 2006b. Diffusion-convection transport of salt solutions in
618 cracked porous building materials. Part 2: Analysis of salt transport in cracked bricks and dead ending cracks.
619 *International Journal for Restoration of Buildings and Monuments* 12 (3), 205-218.
- 620 Prat, M., 1991. 2D modelling of drying of porous media: Influence of edge effects at the interface. *Drying Technology*
621 9 (5), 1181-1208.
- 622 Prat, M., 1993. Percolation model of drying under isothermal conditions in porous media. *International Journal of*
623 *Multiphase Flow* 19 (4), 691-704.
- 624 Prat, M., 2002. Recent advances in pore-scale models for drying of porous media. *Chemical Engineering Journal* 86 (1-
625 2), 153-164.
- 626 Prat, M., 2007. On the influence of pore shape, contact angle and film flows on drying of capillary porous media.
627 *International Journal of Heat and Mass Transfer* 50 (7-8), 1455-1468.
- 628 Putranto, A., Chen, X.D., Devahastin, S., Xiao, Z., Web, P.A., 2011. Application of the reaction engineering approach
629 (REA) for modeling intermittent drying under time-varying humidity and temperature. *Chemical Engineering*
630 *Science* 66 (10), 2149-2156.
- 631 Scheerlinck, N., Verboven, P., Stigter, J., De Baerdemaeker, J., Van Impe, J., Nicolai, B., 2000. Stochastic finite
632 element analysis of coupled heat and mass transfer problems with random field parameters. *Numerical Heat*
633 *Transfer Part b -Fundamentals* 37 (3), 309-330.
- 634 Scheerlinck, N., Verboven, P., Stigter, J., De Baerdemaeker, J., Van Impe, J., Nicolai, B., 2001. A variance propagation
635 algorithm for stochastic heat and mass transfer problems in food processes. *International Journal for Numerical*
636 *Methods in Engineering* 51 (8), 961-983.
- 637 Steeman, H.J., Janssens, A., Carmeliet, J., De Paepe, M., 2009a. Modelling indoor air and hygrothermal wall interaction
638 in building simulation: Comparison between CFD and a well-mixed zonal model. *Building and Environment* 44 (3),
639 572-583.
- 640 Steeman, H.J., Van Belleghem, M., Janssens, A., De Paepe, M., 2009b. Coupled simulation of heat and moisture
641 transport in air and porous materials for the assessment of moisture related damage. *Building and Environment* 44
642 (10), 2176-2184.
- 643 Surasani, V.K., Metzger, T., Tsotsas, E., 2008. Consideration of heat transfer in pore network modelling of convective
644 drying. *International Journal of Heat and Mass Transfer* 51 (9-10), 2506-2518.
- 645 Suresh, H.N., Aswatha Narayana, P.A., Seetharamu, K.N., 2001. Conjugate mixed convection heat and mass transfer in
646 brick drying. *Heat and Mass Transfer* 37 (2-3), 205-213.
- 647 Talukdar, P., Olutmayin, S.O., Osanyintola, O.F., Simonson, C.J., 2007. An experimental data set for benchmarking 1-
648 D, transient heat and moisture transfer models of hygroscopic building materials. Part I: Experimental facility and
649 material property data. *International Journal of Heat and Mass Transfer* 50 (23-24), 4527-4539.

- 650 Turner, I.W., Ilic, M., 1990. Convective drying of a consolidated slab of wet porous material including the sorption
651 region. *International Communications in Heat and Mass Transfer* 17 (1), 39-48.
- 652 van Hooff, T., Blocken, B., 2010. Coupled urban wind flow and indoor natural ventilation modelling on a high-
653 resolution grid: a case study for the Amsterdam ArenA stadium. *Environmental Modelling & Software* 25(1), 51-65.
- 654 Whitaker, S., 1977. Simultaneous heat, mass, and momentum transfer in porous media: A theory of drying. *Advances in*
655 *Heat Transfer* 13, 119-203.
- 656 Whitaker, S., 1998. Coupled transport in multiphase systems: A theory of drying. *Advances in Heat Transfer* 31, 1-104.
- 657 Yang, X., Chen, Q., Zhang, J.S., Magee, R., Zeng, J., Shaw, C.Y., 2001. Numerical simulation of VOC emissions from
658 dry materials. *Building and Environment* 36 (10), 1099-1107.
- 659 Yiotis, A.G., Stubos, A.K., Boudouvis, A.G., Tsimpanogiannis, I.N., Yortsos, Y.C., 2005. Pore-network modelling of
660 isothermal drying in porous media. *Transport in Porous Media* 58 (1-2), 63-86.
- 661 Yiotis, A.G., Stubos, A.K., Boudouvis, A.G., Yortsos, Y.C., 2001. A 2-D pore-network model of the drying of single-
662 component liquids in porous media. *Advances in Water Resources* 24 (3-4), 439-460.
- 663 Yiotis, A.G., Tsimpanogiannis, I.N., Stubos, A.K., Yortsos, Y.C., 2006. Pore-network study of the characteristic periods
664 in the drying of porous materials. *Journal of Colloid and Interface Science* 297 (2), 738-748.
- 665 Younsi, R., Kocaefe, D., Poncsak, S., Kocaefe, Y., 2006. Thermal modelling of the high temperature treatment of wood
666 based on Luikov's approach. *International Journal of Energy Research* 30 (9), 699-711.
- 667 Younsi, R., Kocaefe, D., Poncsak, S., Kocaefe, Y., 2007. Computational modelling of heat and mass transfer during the
668 high-temperature heat treatment of wood, *Applied Thermal Engineering* 27 (8-9), 1424-1431.
- 669 Younsi, R., Kocaefe, D., Poncsak, S., Kocaefe, Y., Gastonguay, L., 2008. CFD modeling and experimental validation of
670 heat and mass transfer in wood poles subjected to high temperatures: a conjugate approach. *Heat and Mass Transfer*
671 44 (12), 1497-1509.
- 672 Zeghmati, B., Daguinet, M., Le Palec, G., 1991. Study of transient laminar free convection over an inclined wet flat
673 plate. *International Journal of Heat and Mass Transfer* 34 (4-5), 899-909.
- 674 Zhai, Z., 2006. Applications of Computational Fluid Dynamics in building design: aspects and trends. *Indoor and Built*
675 *Environment* 15 (4), 305-313.
- 676 Zhai, Z., Chen, Q., Haves, P., Klems, J.H., 2002. On approaches to couple energy simulation and computational fluid
677 dynamics programs. *Building and Environment* 37 (8-9), 857-864.
- 678 Zhai, Z., Chen, Q.Y., 2004. Numerical determination and treatment of convective heat transfer coefficients in the
679 coupled building energy and CFD simulation. *Building and Environment* 39, 1001-1009.
- 680 Zhang, Z., Yang, S., Liu, D., 1999. Mechanism and mathematical model of heat and mass transfer during convective
681 drying of porous materials. *Heat Transfer - Asian Research* 28 (5), 337-351.
- 682

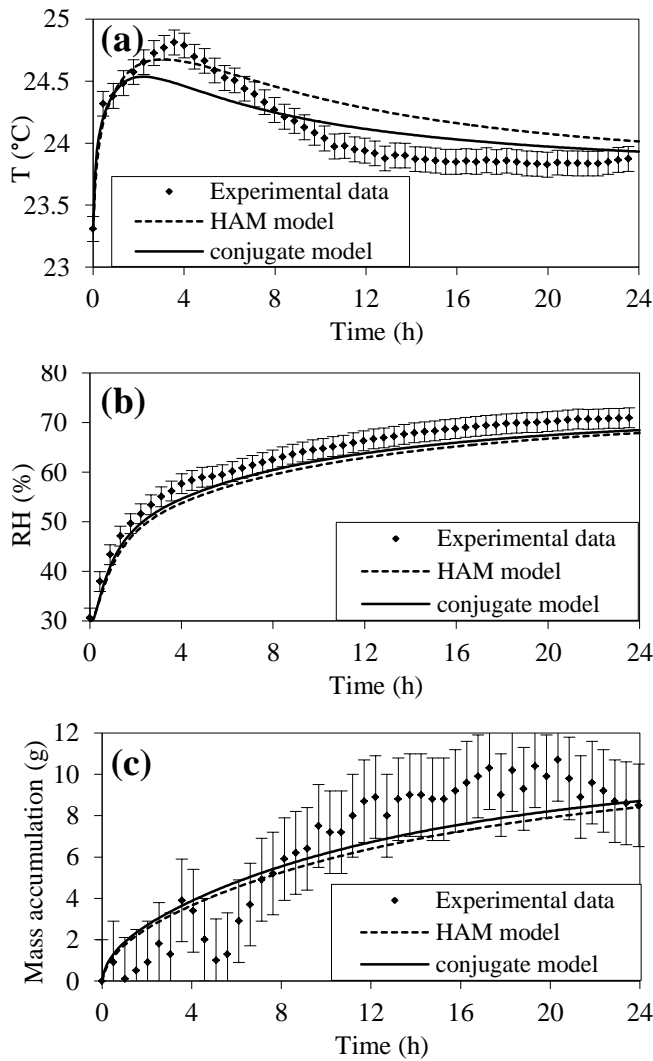
683 **Figure captions**



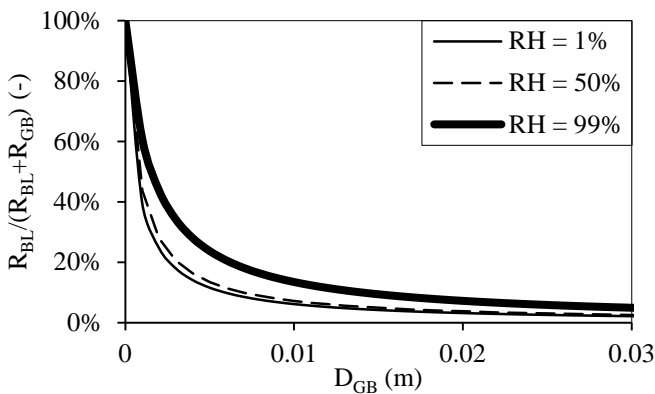
684
 685 **Figure 1. Typical drying rate ($g_{v,w}$), surface temperature (T_w) and relative humidity at the surface (RH_w) of a**
 686 **porous material during drying, as a function of dimensionless time (t/t_{tot}), obtained from a numerical simulation**
 687 **with a porous-material model. The different drying periods are indicated. For $g_{v,w}$ and T_w , scaling is performed**
 688 **using the values during the CDRP (temperatures are in °C). The time is scaled with the total simulation**
 689 **(t_{tot}).**



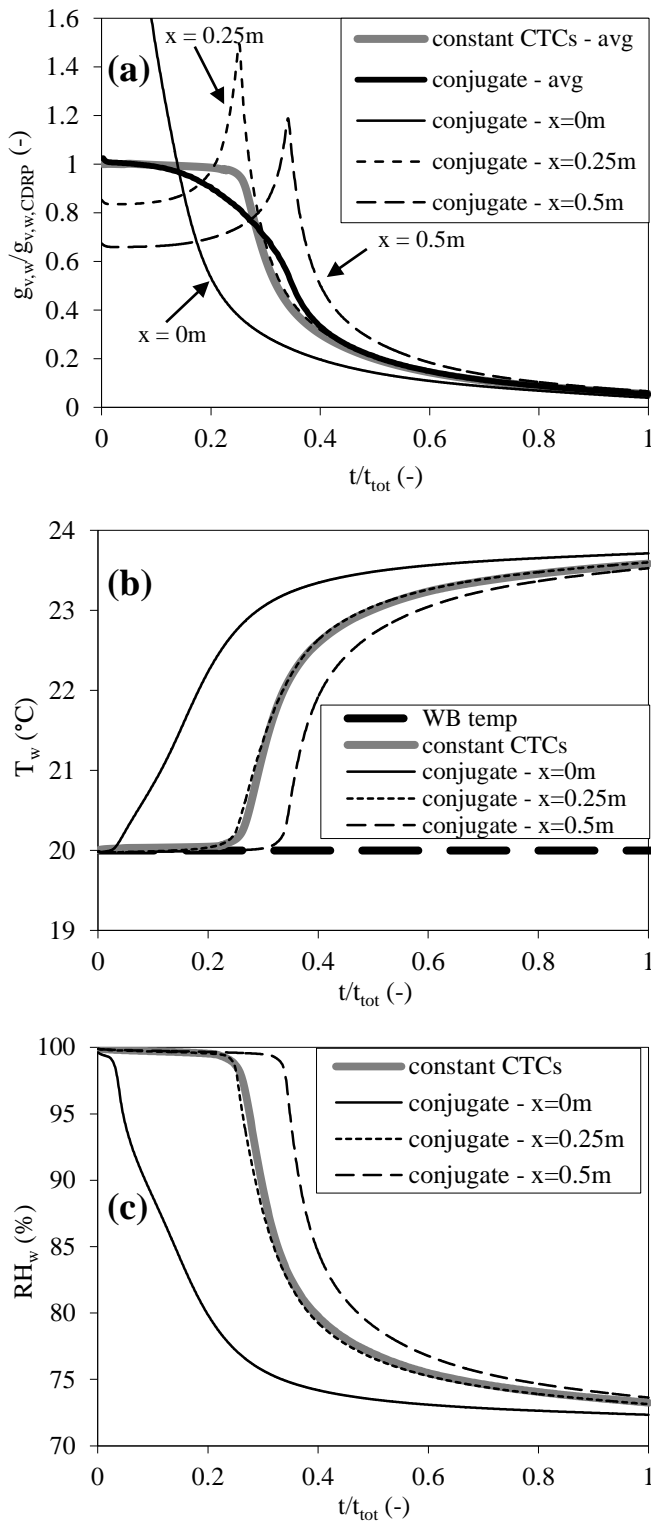
690
 691 **Figure 2. Two-dimensional computational model and boundary conditions for numerical analyses (not to scale,**
 692 **taken from Defraeye et al. 2012; U_b : bulk air speed; H : channel height; Re : Reynolds number based on U_b and**
 693 **H).**



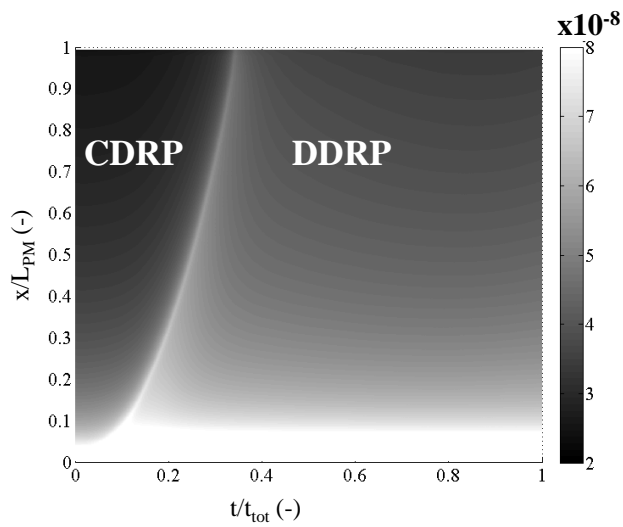
694
 695 **Figure 3. Temperature (a) and relative humidity (b) in the centre of the material below the first gypsum board (x**
 696 **= 250 mm, $y = -12.5$ mm, see Figure 2) as well as the moisture accumulation in the porous material (c), as a**
 697 **function of time: comparison between experiments (with experimental uncertainty, see James et al. 2010),**
 698 **porous-material simulation with constant CTCs (HAM model) and simulation with the conjugate model.**



699
 700 **Figure 4. Boundary-layer vapour transfer resistance (R_{BL}), normalised with the total resistance of the boundary**
 701 **layer and the gypsum board (R_{GB}), as a function of the gypsum board thickness (D_{GB}) for different relative**
 702 **humidities of the gypsum board.**



703
 704 **Figure 5. Comparison of two convective boundary-modelling approaches, namely the constant CTC approach**
 705 **and the conjugate approach, from numerical simulations by Defraeye et al. (2012). For the conjugate approach,**
 706 **parameters at specific locations are given. The time is scaled with the total simulation time (t_{tot}). (a) Drying rate**
 707 **($g_{v,w}$, scaled with $g_{v,w,CDRP}$). The surface-averaged value (avg) for the conjugate approach is also given; (b)**
 708 **Temperature at the interface (T_w). The wet bulb temperature is indicated by WB temp; (c) Relative humidity at**
 709 **the interface (RH_w).**



710

711 **Figure 6. CMTC, as a function of time (scaled with t_{tot}) and location on the surface (scaled with L_{PM}), calculated**
712 **according to the conjugate approach, from numerical simulations by Defraeye et al. (2012). The CDRP and**
713 **DDRP are indicated.**

714

Defraeye T., Blocken B., Derome D., Nicolai B., Carmeliet J., (2012), Convective heat and mass transfer modelling at air-porous material interfaces: overview of existing methods and relevance, *Chemical Engineering Science* 74, 49-58. <http://dx.doi.org/10.1016/j.ces.2012.02.032>

715 **Table captions**

716

717 **Table 1. Overview of numerical modelling research of porous materials using conjugate convective heat and**
718 **mass transfer modelling.**

719

Author(s)	Porous material	Fluid flow	Coupling	Porous material modelling	Fluid flow modelling	Dim.	Validation
Chen and Pei (1989)	Wool bobbins, brick slabs and corn kernels, Sat.	($U_{\infty}=2.33\text{-}5.25\text{m/s}$, $T_{\infty}=71\text{-}80^{\circ}\text{C}$)	FC*	SCM (FE) (†)	CTCs (‡)	1D	Yes (‡) (†)
Masmoudi and Prat (1991)	PM (0.1mx0.1m), Unsat.	Lam. Forc. ($U_{\infty}=1\text{m/s}$, $T_{\infty}=25^{\circ}\text{C}$)	FC*	H&M TEq. (FE)	CTCs (‡)	2D	No
Zeghmami et al. (1991)	capillary PM, Sat.	Lam. Nat.	FC	H&M TEq. (FD)	BL Eqs. (FD) Trans.	2D	Yes (‡) (†)
Dolinskiy et al. (1991)	Paper, Sat.	Lam. Forc. ($T_{\infty}=90^{\circ}\text{C}$)	FC	H&M TEq. (FD)	BL Eqs. (FD) Trans.	2D	No
Oliveira et al. (1994)	Corn meal plate (0.02mx0.02m), Sat.	Lam. Nat.	SC (†)	H&M TEq. (FV)	BL Eqs. (FD) Steady	2D	No
Oliveira and Haghighi (1998)	Wood board sample (0.1mx0.025m), Unsat.	Lam. Forc. ($Re=200$, $T_{\infty}=60^{\circ}\text{C}$)	SC	H&M TEq. (FE)	Nav.-Stok. (FE) Steady	2D	No
Suresh et al. (2001)	Brick (0.2mx0.1m), Sat.	Lam. Mix. ($U_{\infty}=0.03\text{m/s}$, $T_{\infty}=30^{\circ}\text{C}$)	FC	H&M TEq. (FE)	Nav.-Stok. (FE) Trans.	2D	Yes (‡) (†)
Murugesan et al. (2001)	Brick (0.2mx0.1m), Sat.	Lam. Mix. ($U_{\infty}=0.03\text{m/s}$, $T_{\infty}=20^{\circ}\text{C}$)	SC	H&M TEq. (FE)	Nav.-Stok. (FE) Steady	2D	Yes (‡) (†)
Erriguible et al. (2005, 2006)	Wood (0.01mx0.01m), Sat.	Turb. Mix. ($U_{\infty}=0.5\text{m/s}$, $T_{\infty}=60^{\circ}\text{C}$)	FC (†)	H&M TEq. (FE) (†)	Nav.-Stok. (FV) Trans.	2D	No
Kaya et al. (2006)	Rectangular cylinders (apple slices) (0.02mx0.08m), Sat.	Turb. Mix. ($U_{\infty}=0.33\text{m/s}$, $T_{\infty}=50^{\circ}\text{C}$)	UC	H&M TEq. (FD)	Nav.-Stok. (FV) Trans. vortex shedding	2D	Yes (†)
Younsi et al. (2007)	Wood (0.035mx0.035mx0.2m), Unsat.	Lam. Mix. ($U_{\infty}=0.02\text{-}1\text{m/s}$, $T_{\infty}=20\text{-}220^{\circ}\text{C}$)	FC	H&M TEq. (FE) (†)	Nav.-Stok. (FE) Trans.	3D	Yes
Mortensen et al. (2007)	Cellular concrete wall in a room (Thickness 0.1m), Unsat.	Turb. ($U_{inlet}=0.056\text{-}0.33\text{m/s}$, $T_{inlet}=20^{\circ}\text{C}$)	FC**	H&M TEq. (FV)	Nav.-Stok. (FV) Steady	3D	Yes (‡) (†)
Younsi et al. (2008)	Wood (0.1mx0.1mx2m), Unsat.	Turb. Forc. ($U_{\infty}=5\text{m/s}$, $T_{\infty}=10\text{-}220^{\circ}\text{C}$)	FC	H&M TEq. (FD) (†)	Nav.-Stok. (FV) Trans.	3D	Yes
De Bonis and Ruocco (2008)	Rectangular carrot slice (0.06mx0.015m), Unsat.	Lam. Forc. ($U_{\infty}=0.3\text{m/s}$, $T_{\infty}=80^{\circ}\text{C}$)	FC	H&M TEq. (FE)	Nav.-Stok. (FE) Trans.	2D	Yes (†)
Lamnatou et al. (2009)	Rectangular cylinder (apple slice) (0.25mx0.05m), Sat.	Lam. Forc. ($U_{\infty}=0.33\text{-}0.67\text{m/s}$, $T_{\infty}=50^{\circ}\text{C}$)	FC	H&M TEq. (FV)	Nav.-Stok. (FV) Trans.	2D	Yes (‡) (†)
Steehan et al. (2009a)	Cellular concrete wall in a room (Thickness 0.1m), Unsat.	Turb. Mix. ($T_{inlet}=11\text{-}20.4^{\circ}\text{C}$)	FC	Heat TEq. (FV) - Mass EPDM	Nav.-Stok. (FV) Trans.	2D/ 3D(*)	Yes (‡) (†)
Steehan et al. (2009b)	Microclimate vitrine for paintings, Unsat.	Lam. Nat.	FC (†)	H&M TEq. (FV)	Nav.-Stok. (FV) Trans.	3D	Yes (†)
Lamnatou et al. (2010)	Rectangular cylinders (apple slices) (0.25mx0.05m), Sat.	Lam. Forc. ($Re=463\& 926$, $T_{\infty}=50^{\circ}\text{C}$)	FC	H&M TEq. (FV)	Nav.-Stok. (FV) Trans.	2D	Yes (‡) (†)
Chandra Mohan and Talukdar (2010)	Rectangular cylinder (0.02mx0.02mx0.08m), Sat.	Lam. Forc. ($U_{\infty}=0.1\text{-}0.3\text{m/s}$, $T_{\infty}=40\text{-}80^{\circ}\text{C}$)	UC	H&M TEq. (FV)	Nav.-Stok. (FV) Steady	3D	Yes (‡) (†)
Defraeye et al. (2012)	Mineral plaster plate (0.5mx0.0375m), Unsat.	Lam. Forc. ($Re=1100$, $T_{\infty}=23.8^{\circ}\text{C}$)	FC (†)	H&M TEq. (FE)	Nav.-Stok. (FV) Trans.	2D	Yes (‡) (†)

BL Eqs.: Boundary-layer equations, **Dim.:** Dimension (1D, 2D, 3D), **EPDM:** Effective Penetration Depth Model, **FC:** Full coupling (PM and flow field are both solved each time step), **FC*:** Full coupling (PM and CTCs are both solved each time step, where CTCs are dependent on PM conditions), **FC**:** Full coupling (PM and flow field are both solved but in steady state), **FD:** Finite Difference method, **FE:** Finite Element method, **FV:** Finite Volume method, **Forc.:** Forced convection, **H&M:** Heat and mass transfer, **Lam.:** Laminar flow, **Mix.:** Mixed convection, **Nat.:** Natural convection, **Nav.-Stok.:** Navier-Stokes equations, **PM:** Porous material, **Sat.:** Saturated PM, **SC:** Semicoupled (Fluid flow is solved assuming a quasi-steady flow field but transport of heat and moisture in the flow field is calculated every time step, as well as the PM), **SCM:** Shrinking Core Model, **Steady:** Fluid flow is assumed to be quasi-steady and is thereby taken constant in time and is thus not coupled with the PM calculation and is consequently only solved once (i.e. not every time step), **TEq.:** Transport equations, **Trans.:** Transient flow calculation (i.e. performed for each time step), **Turb.:** Turbulent flow, **UC:** Uncoupled approach (CTCs from separate CFD simulation and these are afterwards transferred to porous-material model), **Unsat.:** Unsaturated PM; (*): Validation was performed separately for the flow field and the PM, (†): Validation was only performed for the porous material, (‡): Validation was only performed for the flow field, (‡): Validation was performed with data from other researchers, (*): 3D for flow and 2D for PM, (†): PM and flow field are solved using two different programs where BC information is exchanged between programs every time step, (‡): CTCs vary with the moisture content in the decreasing drying rate period, (‡): Local CTCs obtained with superposition method (Kays and Crawford 1993, pp. 175-178) for each time step, (†): Bound water taken into account, (†): PM and flow field are solved using two different programs where during each time step iterations are performed between both programs until convergence is reached within that time step, (‡): Radiation is taken into account, (†) Validation of the models that are used was performed in previous studies.